



Novel Proportionate Adaptive Filters with Coefficient Vector Reusing

José V. G. de Souza¹ · Diego B. Haddad² · Felipe da R. Henriques² · Mariane R. Petraglia³

Received: 5 September 2018 / Revised: 15 September 2019 / Accepted: 16 September 2019 /
Published online: 25 September 2019
© Springer Science+Business Media, LLC, part of Springer Nature 2019

Abstract

In this paper, a new family of adaptive filtering algorithms is presented, which aims to combine the small misalignment resulting from the reuse of past weight vectors with the fast convergence arising from the proportionate adaptation and logarithmic cost functions. This family of algorithms is obtained as a solution to a deterministic constrained optimization problem, by using the Lagrange multipliers technique, which differs from the traditionally employed stochastic gradient technique. Two special cases are proposed, namely the improved mu-law proportionate least mean logarithmic square with reuse of coefficients (IMPLMLS-RC) algorithm and the improved mu-law proportionate least logarithmic absolute difference with reuse of coefficients (IMPLLAD-RC) algorithm. An energy conservation relationship is established, which can be employed to perform stochastic transient analyses of the proposed algorithms. Simulations in system identification and active noise control applications show the advantages of the IMPLMLS-RC and IMPLLAD-RC algorithms over the traditional LMS and LAD, and the recently proposed LMLS and LLAD, with respect to both steady-state performance and robustness against impulsive noise.

Keywords Adaptive filter · Coefficient vector reusing · LMS algorithm · LAD algorithm

1 Introduction

Adaptive filters have been effectively applied in a wide range of challenging tasks such as system identification, channel equalization, active noise control (ANC) and echo cancelation [8]. In system identification, the objective of an adaptive filter, shown in Fig. 1, is to iteratively update the vector $\mathbf{w}(k) \in \mathbb{R}^N$ to approach the unknown

This work was supported in part by Conselho Nacional de Desenvolvimento Científico e Tecnológico and in part by Fundação Carlos Chagas Filho de Amparo a Pesquisa do Estado do Rio de Janeiro.

Extended author information available on the last page of the article

Fig. 1 Block diagram of the system identification problem

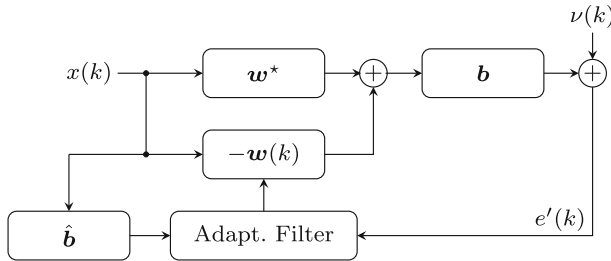
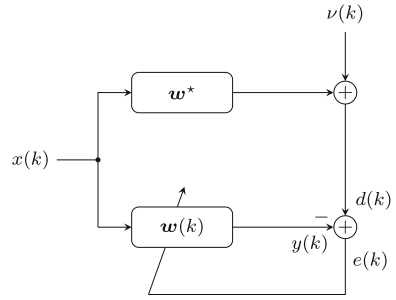


Fig. 2 Block diagram of the ANC problem, where \hat{b} denotes an estimate of the secondary path b

vector $\mathbf{w}^* \in \mathbb{R}^N$, whose elements contain the coefficients of a transfer function to be emulated. The identification process intends to progressively reduce, in statistical terms, the quadratic error $e^2(k)$, with the error defined as

$$e(k) \triangleq d(k) - y(k), \tag{1}$$

where $y(k) \triangleq \mathbf{w}^T(k)\mathbf{x}(k)$ is the filter output at the k th iteration, $d(k) = \mathbf{x}^T(k)\mathbf{w}^*\mathbf{x}(k) + \nu(k)$ is the reference signal, $\mathbf{x}(k) \in \mathbb{R}^N$ is the input signal and $\nu(k)$ accounts for both model imprecisions and measurement noise.

ANC systems consist of a powerful tool for several practical problems that involve the introduction of secondary sources driven so that the field generated by these sources interferes destructively with the field caused by the original source [6,10,13–16]. Commonly, they employ adaptive FIR filters trained with the filtered-x LMS algorithm [6] for both internal model control and feedforward systems [3]. Usually, the secondary path is estimated online by the injection of auxiliary noise [4]. With respect to the characteristics of the targeted noise, the active noise control arises in two flavors: the broadband ANC and the narrowband ANC [29]. Figure 2 presents the structure of a typical scheme proper for ANC tasks.

We emphasize the least mean squares (LMS) and the normalized least mean squares (NLMS) [8] among classical adaptive filtering algorithms. The LMF (least mean fourth) algorithm proposed in [28] shows in some circumstances a better convergence than that of the LMS approach, although it often presents stability problems. A logarithmic cost function is proposed in [25], from which the least mean logarithmic square (LMLS) and least logarithmic absolute difference (LLAD) algorithms are

derived by means of a stochastic gradient method. The LLAD is more robust than the LMS in scenarios subject to impulsive noise and outperforms the LAD algorithm [25].

It is noteworthy that the coefficient reuse technique minimizes the weighted sum of the squares of the Euclidean distances among the actual vector of adaptive coefficients $\mathbf{w}(k+1)$ and the L past vectors $\mathbf{w}(k-l)$, with $l \in \{0, 1, \dots, L-1\}$, where L is a parameter chosen by the designer [11]. Such technique is able to enhance the steady-state performance in low-SNR scenarios [5, 18–23].

Each adaptive coefficient of proportionate adaptation algorithms has its learning factor adjusted by its relative magnitude. According to the estimated sparsity of the transfer function to be identified, these algorithms achieve a faster convergence than traditional algorithms when the channel to be identified is sparse [17]. However, for scattered channels, their performances may be substantially reduced [7]. A modified version of the proportionate algorithm presented in [2] is proposed in [12] to estimate the sparsity of a channel to be identified, by automatically adjusting the distribution of the updating energy among several adaptive coefficients, and allowing a convergence rate that is comparable to the traditional algorithms for dispersive channels. Proportionate adaptation algorithms are employed in this work because they tend to compensate lower convergence rates by considering the reuse of data that is also adopted in view of its better steady-state performance.

This paper presents the derivation of the LMLS and LLAD algorithms from the exact solution of a local deterministic optimization problem, which differs from the originally employed stochastic gradient technique. This new paradigm allows the achievement of general versions of these algorithms, by employing coefficient reuse and proportionate adaptation approaches. Thus, we also derive the following algorithms: improved mu-law least mean logarithmic square with reuse of coefficients (IMPLMLS-RC) and improved mu-law least logarithmic difference with reuse of coefficients (IMPLLAD-RC). These approaches intend to increase the performance of LMLS and LLAD algorithms, incorporating both coefficient reuse techniques presented in [5] and the proportionate adaptation scheme suggested in [12].

This work is structured as follows: Sect. 2 describes the LMLS and LLAD algorithms and provides a deterministic optimization framework which unifies the derivation of such methods; the proposed proportionate adaptive algorithms with coefficient vector reusing are derived in Sect. 3; an energy-based relationship, which can be used to perform a stochastic transient analysis of the proposed algorithms, is derived in Sect. 4; simulation setup and results are discussed in Sect. 5; conclusions are presented in Sect. 6.

2 LMLS and LLAD Algorithms

As presented in [25], both LMLS and LLAD algorithms are derived from the following cost function

$$\mathcal{J}[e(k)] \triangleq \mathcal{F}[e(k)] - \frac{1}{\alpha} \ln(1 + \alpha \mathcal{F}[e(k)]), \quad (2)$$

where $\alpha > 0$ is a design parameter and $\mathcal{F}[e(k)]$ is the traditional cost function that generally depends on $e(k)$, just like $\mathbb{E}[e^2(k)]$, in which $\mathbb{E}[\cdot]$ denotes the statistical

mean operator. Starting from the gradient of $\mathcal{J}[e(k)]$ with respect to $\mathbf{w}(k)$ and by the computation of the stochastic approximation that replaces $\mathcal{F}[e(k)]$ by $f(e(k))$ (i.e., $\mathcal{F}[e(k)] = \mathbb{E}[f(e(k))]$), the coefficient updating equation of $\mathbf{w}(k)$ is given by [25]:

$$\mathbf{w}(k+1) = \mathbf{w}(k) + \beta \mathbf{x}(k) \frac{\partial f(e(k))}{\partial e(k)} \frac{\alpha f(e(k))}{1 + \alpha f(e(k))}, \quad (3)$$

where β is the learning factor, which provides a trade-off among convergence rate, steady-state performance and probability of instability. By choosing $f(e(k)) = e^2(k)$, the LMLS algorithm

$$\mathbf{w}(k+1) = \mathbf{w}(k) + \beta \frac{\alpha \mathbf{x}(k) e^3(k)}{1 + \alpha e^2(k)} \quad (4)$$

is obtained, and assuming $f(e(k)) = |e(k)|$ the LLAD algorithm

$$\mathbf{w}(k+1) = \mathbf{w}(k) + \beta \frac{\alpha \mathbf{x}(k) e(k)}{1 + \alpha |e(k)|} \quad (5)$$

is derived. In [25], the updating equations were obtained by a stochastic argument, replacing the expectation $\mathbb{E}[e^2(k)]$ by $e^2(k)$, for example. It is known that the *diminishing return* functions employed in (5)–(4) tend to improve the convergence performance [26].

Next, we present a new derivation for the LMLS and LLAD algorithms through a minimal perturbation approach, along with additional constraints. Besides being a tool that enables the development of new algorithms, the proposed unified optimization framework provides insight into their expected behavior.

The update Eqs. (4) and (5) can be derived by solving the deterministic optimization problem

$$\begin{aligned} \min_{\mathbf{w}(k+1)} \quad & \|\mathbf{w}(k+1) - \mathbf{w}(k)\|^2 \\ \text{s.t.} \quad & e_p(k) = (1 - g[e(k)]) e(k), \end{aligned} \quad (6)$$

where the *a posteriori* error $e_p(k)$ is defined by

$$e_p(k) \triangleq d(k) - \mathbf{w}^T(k+1) \mathbf{x}(k). \quad (7)$$

The function $g[e(k)]$ is

$$g_{\text{LMLS}}[e(k)] = \beta \frac{\alpha \|\mathbf{x}(k)\|^2 e^2(k)}{1 + \alpha e^2(k)} \quad (8)$$

and

$$g_{\text{LLAD}}[e(k)] = \beta \frac{\alpha \|\mathbf{x}(k)\|^2}{1 + \alpha |e(k)|} \quad (9)$$

for the LMLS and LLAD, respectively. It should be noted that the choices

$$g_{\text{LMS}}(e(k)) = \beta \|\mathbf{x}(k)\|^2, \quad (10)$$

$$g_{\text{LMF}}(e(k)) = \beta \|\mathbf{x}(k)\|^2 e^2(k), \quad (11)$$

and

$$g_{\text{LAD}}(e(k)) = \frac{\beta \|\mathbf{x}(k)\|^2 e^2(k)}{|e(k)|} \quad (12)$$

give place to the LMS, LMF and LAD algorithms, respectively [24]. Functions $g_{\text{LMLS}}(e(k))$ and $g_{\text{LLAD}}(e(k))$ combine the higher- and lower-order measures of the error, which allows the use of higher-order statistics of the errors when the perturbations are small [26]. It can be observed that the LMLS behaves as the LMF when the error is small, which enhances its convergence, and as the LMS when the error is large, which avoids the stability issues of LMF [25]. Similarly, the LLAD maintains the robustness of the LAD in scenarios having impulsive noise, since $g_{\text{LLAD}}(e(k))$ approximates $g_{\text{LAD}}(e(k))$ in high-magnitude error regime, thereby presenting better convergence properties than those of the LAD, since $g_{\text{LLAD}}(e(k))$ tends to $g_{\text{LMS}}(e(k))$ when the error is small.

3 Proposed Algorithms

The main contribution of this paper is to derive generalized versions of LMLS and LLAD algorithms, by employing coefficient reuse and proportionate adaptation, which can be interpreted as solvers of a *deterministic* (instead of stochastic) optimization problem. In mathematical terms, let

$$\mathcal{G}[\bar{e}(k)] \triangleq (1 - g[\bar{e}(k)]) \bar{e}(k) \quad (13)$$

be the constraint for the a posteriori error $e_p(k)$, with $\bar{e}(k)$ defined by

$$\bar{e}(k) \triangleq d(k) - \frac{1 - \rho}{1 - \rho^L} \sum_{l=0}^{L-1} \rho^l \mathbf{w}^T(k-l) \mathbf{x}(k), \quad (14)$$

where L is the length of the reuse window of the past adaptive coefficients¹ and $0 < \rho < 1$ is a parameter that balances the steady-state performance and the convergence rate.² The proposed family of proportionate adaptive algorithms with reusing coefficients vector can thus be obtained from the local optimization problem

¹ Increasing L enhances the steady-state performance, which is important when the SNR is low [5], at the cost of reducing the convergence rate.

² Choosing a small ρ is equivalent to emphasizing the most recent adaptive coefficient vectors. In the case of $\rho \rightarrow 1$, the last L estimated vectors assume similar importance.

$$\begin{aligned} \min \quad & \frac{1}{2} \sum_{l=0}^{L-1} \rho^l \|\mathbf{w}(k+1) - \mathbf{w}(k-l)\|_{\mathbf{\Lambda}^{-1}(k)}^2 \\ \text{s.t.} \quad & e_p(k) = \mathcal{G}[\bar{e}(k)], \end{aligned} \tag{15}$$

in which $\|\mathbf{x}\|_{\mathbf{\Lambda}}^2 \triangleq \mathbf{x}^T(k)\mathbf{\Lambda}\mathbf{x}(k)$, $\|\cdot\|^2$ stands for the Euclidean norm and $\mathbf{\Lambda}(k)$ is a diagonal matrix, whose main diagonal elements adjust the learning rate of each coefficient, by means of the proportionate adaptation principle [12], so that coefficients with larger magnitude have a stronger update.

The usage of the Lagrange multipliers technique allows the derivation of a function, whose minimum value matches with the solution of the original optimization problem (15), given by

$$\begin{aligned} \mathcal{F}[\mathbf{w}(k+1)] = & \frac{1}{2} \sum_{l=0}^{L-1} \rho^l \|\mathbf{w}(k+1) - \mathbf{w}(k-l)\|_{\mathbf{\Lambda}^{-1}(k)}^2 \\ & + \lambda [e_p(k) - (1 - g[\bar{e}(k)])\bar{e}(k)]. \end{aligned}$$

The minimization of $\mathcal{F}[\mathbf{w}(k+1)]$ with respect to $\mathbf{w}(k+1)$ yields

$$\begin{aligned} \frac{\partial \mathcal{F}[\mathbf{w}(k+1)]}{\partial \mathbf{w}(k+1)} = & \mathbf{\Lambda}^{-1}(k)\mathbf{w}(k+1) \left(\frac{1 - \rho^L}{1 - \rho} \right) \\ & - \mathbf{\Lambda}^{-1}(k) \sum_{l=0}^{L-1} \rho^l \mathbf{w}(k-l) - \lambda \mathbf{x}(k) = \mathbf{0}. \end{aligned}$$

We thus conclude that the form of the updating equation is described by

$$\begin{aligned} \mathbf{w}(k+1) = & \frac{1 - \rho}{1 - \rho^L} \sum_{l=0}^{L-1} \rho^l \mathbf{w}(k-l) \\ & + \frac{1 - \rho}{1 - \rho^L} \lambda \mathbf{\Lambda}(k)\mathbf{x}(k). \end{aligned} \tag{16}$$

Applying (16) to constraint (13) and employing (14) leads to

$$\frac{1 - \rho}{1 - \rho^L} \lambda = \frac{g[\bar{e}(k)]\bar{e}(k)}{\|\mathbf{x}(k)\|_{\mathbf{\Lambda}(k)}^2}. \tag{17}$$

Combining (16) and (17), we obtain the final updating equation

$$\begin{aligned} \mathbf{w}(k+1) = & \frac{1 - \rho}{1 - \rho^L} \sum_{l=0}^{L-1} \rho^l \mathbf{w}(k-l) \\ & + \frac{\mathbf{\Lambda}(k)\mathbf{x}(k)g[\bar{e}(k)]\bar{e}(k)}{\|\mathbf{x}(k)\|_{\mathbf{\Lambda}(k)}^2}, \end{aligned} \tag{18}$$

which is a very general update scheme that incorporates coefficients reuse and proportionate adaptation. It is noteworthy that the optimization problem (15) is equivalent to a convex quadratic programming with a one-dimensional affine subspace, and hence, its solution presents a closed-form expression.

The computational burden involved in the evaluation of the term

$$\phi(k) \triangleq \frac{\overbrace{1-\rho}^{\triangleq \theta(\rho)}}{1-\rho^L} \sum_{l=0}^{L-1} \rho^l \mathbf{w}(k-l) \tag{19}$$

can be alleviated by using the recursion

$$\phi(k+1) = \theta(\rho)\mathbf{w}(k+1) + \rho\phi(k) - \theta(\rho)\rho^L\mathbf{w}(k-L+1), \tag{20}$$

which implies that the referred burden related to this term does not increase with L .

It is straightforward to verify that the simple choice (SC) configuration defined by $L = 1$, $\rho \rightarrow 1$ and $\mathbf{A}(k) = \mathbf{I}_N$ (i.e., the identity matrix), which leads to $\bar{e}(k) = e(k)$, together with the use of the $g[e(k)]$ functions selected in (8) and (9), generates the LMLS and LLAD algorithms, which can be regarded as solvers of particular cases of the optimization problem described by (15).

Although $\mathbf{A}(k)$ may assume the identity matrix, it is possible to choose more appropriate main diagonal elements in order to increase the convergence rate. According to [12], these elements are determined from the estimation of the channel sparsity ξ , defined by

$$\xi(k) = (1 - \eta)\xi(k - 1) + \eta\xi_{\mathbf{w}}(k), \quad 0 < \eta \ll 1, \tag{21}$$

in which η is a fading factor and $\xi_{\mathbf{w}}(k)$ is defined by

$$\xi_{\mathbf{w}}(k) \triangleq \frac{N}{N - \sqrt{N}} \left(1 - \frac{\|\mathbf{w}(k)\|_1}{\sqrt{N}\|\mathbf{w}(k)\|_2} \right), \tag{22}$$

where N is the number of channel coefficients. Finally, the estimated sparsity $\xi(k)$ is mapped to the parameter $\gamma(k) \triangleq 2\xi(k) - 1$ and the elements of the main diagonal of $\mathbf{A}(k)$ are given by

$$\lambda_n(k) \triangleq \frac{1 - \gamma(k)}{2N} + \frac{(1 + \gamma(k))G(|w_n(k)|)}{2\|G(|\mathbf{w}(k)|)\|_1 + \epsilon}, \tag{23}$$

where ϵ is a regularization constant and $G(|w_n(k)|)$ is defined by [12]

$$G(|w_n(k)|) \triangleq \begin{cases} 400|w_n(k)|, & |w_n(k)| < 0.005 \\ 8.51|w_n(k)| + 1.96, & \text{otherwise.} \end{cases} \tag{24}$$

4 Energy Conservation Relationship

Energy conservation arguments can be employed to predict the performance of adaptive algorithms [1,30]. Let

$$\tilde{\mathbf{w}}(k+1) \triangleq \mathbf{w}^* - \mathbf{w}(k), \quad (25)$$

be the deviation vector. The general update Eq. (18) can be rewritten as

$$\tilde{\mathbf{w}}(k+1) = \theta(\rho) \sum_{l=0}^{L-1} \rho^l \tilde{\mathbf{w}}(k-l) - \frac{\mathbf{\Lambda}(k)\mathbf{x}(k)g(\cdot)e(k)}{\|\mathbf{x}(k)\|_{\mathbf{\Lambda}(k)}^2}. \quad (26)$$

Let us define the error-related quantities

$$e_p^{\Sigma}(k) \triangleq \mathbf{x}^T(k) \Sigma \tilde{\mathbf{w}}(k+1), \quad (27)$$

$$e_{a,l}^{\Sigma}(k) \triangleq \mathbf{x}^T(k) \Sigma \tilde{\mathbf{w}}(k-l), \quad \text{for } l \in \{0, 1, \dots, L-1\}, \quad (28)$$

where $\Sigma \in \mathbb{R}^{N \times N}$ is an arbitrary symmetric matrix. Premultiplying both sides of (26) by $\mathbf{x}^T(k) \Sigma$ yields

$$e_p^{\Sigma}(k) = \theta(\rho) \sum_{l=0}^{L-1} \rho^l e_{a,l}^{\Sigma}(k) - \frac{\|\mathbf{x}(k)\|_{\Sigma \mathbf{\Lambda}(k)}^2}{\|\mathbf{x}(k)\|_{\mathbf{\Lambda}(k)}^2} g(\cdot)e(k). \quad (29)$$

By isolating $g(\cdot)e(k)$ in (29) and substituting this term in (26), we obtain

$$\begin{aligned} \tilde{\mathbf{w}}(k+1) + \theta(\rho) \mathbf{\Lambda}(k)\mathbf{x}(k) \sum_{l=0}^{L-1} \rho^l \frac{e_{a,l}^{\Sigma}(k)}{\|\mathbf{x}(k)\|_{\Sigma \mathbf{\Lambda}(k)}^2} \\ = \theta(\rho) \sum_{l=0}^{L-1} \rho^l \tilde{\mathbf{w}}(k-l) + \frac{\mathbf{\Lambda}(k)\mathbf{x}(k)e_p^{\Sigma}(k)}{\|\mathbf{x}(k)\|_{\Sigma \mathbf{\Lambda}(k)}^2}. \end{aligned} \quad (30)$$

By evaluating the energy of both sides of (30), as advanced in [11,27], the following identity is established:

$$\begin{aligned} \|\tilde{\mathbf{w}}(k+1)\|^2 + \theta(\rho) e_p^{\mathbf{\Lambda}(k)} \sum_{l=0}^{L-1} \frac{\rho^l e_{a,l}^{\Sigma}(k)}{\|\mathbf{x}(k)\|_{\Sigma \mathbf{\Lambda}(k)}^2} \\ + \theta^2(\rho) \|\mathbf{x}(k)\|_{\mathbf{\Lambda}^2(k)}^2 \sum_{l_1=0}^{L-1} \sum_{l_2=0}^{L-1} \frac{\rho^{l_1} \rho^{l_2} e_{a,l_1}^{\Sigma}(k) e_{a,l_2}^{\Sigma}(k)}{\|\mathbf{x}(k)\|_{\Sigma \mathbf{\Lambda}(k)}^4} \\ = \theta^2(\rho) \sum_{l_1=0}^{L-1} \sum_{l_2=0}^{L-1} \rho^{l_1} \rho^{l_2} \tilde{\mathbf{w}}^T(k-l_1) \tilde{\mathbf{w}}(k-l_2) \end{aligned}$$

$$+ \theta(\rho) e_p^{\Sigma}(k) \sum_{l=0}^{L-1} \rho^l \frac{e_{a,l}^{\Sigma(k)}(k)}{\|\mathbf{x}(k)\|_{\Sigma \Lambda(k)}^2} + \frac{\left[e_p^{\Sigma}(k) \right]^2 \|\mathbf{x}(k)\|_{\Lambda(k)}^2}{\|\mathbf{x}(k)\|_{\Sigma \Lambda(k)}^4}, \quad (31)$$

which can be employed to perform an exact stochastic transient analysis of the proposed algorithm, using the usual procedures of the energy-based approach [27]. It is noteworthy that in the case of steady-state analysis, the choice $\Sigma = \Lambda_k$ simplifies (31).

5 Simulation Results

In the following, the mean-square deviation, defined by

$$\text{MSD (dB)} \triangleq 10 \log_{10} \|\mathbf{w}^* - \mathbf{w}(k)\|^2, \quad (32)$$

is adopted as the metric to evaluate the performance of the proposed algorithms.

5.1 System Identification

In order to measure the performance of the proposed algorithms, we run simulations with two groups of algorithms. For both groups, we consider the following setup: $\mathbf{x}(k)$ as the white Gaussian input signal with zero mean and variance equal to one; \mathbf{w}^* as the 64-length channel (model 1 of [9]); white Gaussian measuring noise with zero mean and variance $\sigma_v^2 = 0.01$.

The first group of algorithms is composed of LMS, LMLS and IMPLMLS-RC. We assumed the values $\epsilon = 10^{-6}$ for the regularization factor and $\eta = 0.1$ for the fading factor, for all the algorithms proposed in this paper. Figures 3 and 4 show the MSD obtained by 100 Monte Carlo independent runs for these three algorithms. The parameters used in the simulations of Figs. 3 and 4 are listed in Tables 1 and 2, respectively. Those values were chosen so that all algorithms had similar steady-state MSD, thereby allowing a fair comparison. Moreover, simulation results with $L = 5$ and $L = 10$ are also presented in Fig. 3 in order to show the reuse window length effects on the performance of the proposed algorithm. It can be verified that larger values of L tend to improve steady-state MSD while keeping the convergence rate competitive with respect to the LMLS algorithm. Simulation results for $\rho = 0.7$ and $\rho = 0.1$, with $L = 2$, are also shown in Fig. 4. It can be observed that as ρ decreases, the convergence rate improves, while matching steady-state MSD of the LMLS and LMS algorithms. Table 3 presents the iteration number for which the MSD of each algorithm has converged.

The second group of algorithms consists of LAD, LLAD and IMPLLAD-RC. A Gaussian impulsive noise with zero mean, variance $\sigma^2 = 10^8$ and probability of occurrence of 0.01 was added to the desired signal ($d(k)$) with the simulation conditions employed for the first group. Figures 5 and 6 show comparisons among the algorithms from the second group. The parameter values shown used in these simulations are presented in Tables 4 and 5. These values were chosen in order to guarantee a similar

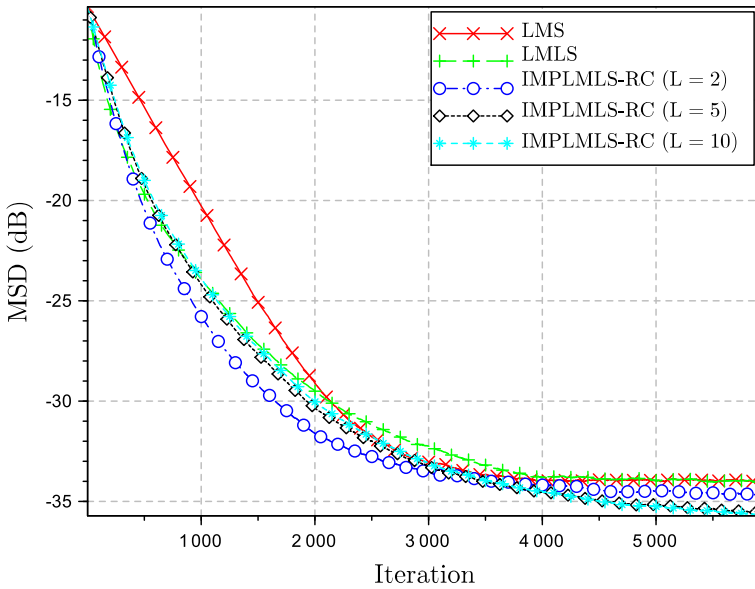


Fig. 3 Comparisons among the LMS, LMLS and IMPLMLS-RC algorithms for $\rho = 0.45$, $L = 2$, $L = 5$ and $L = 10$

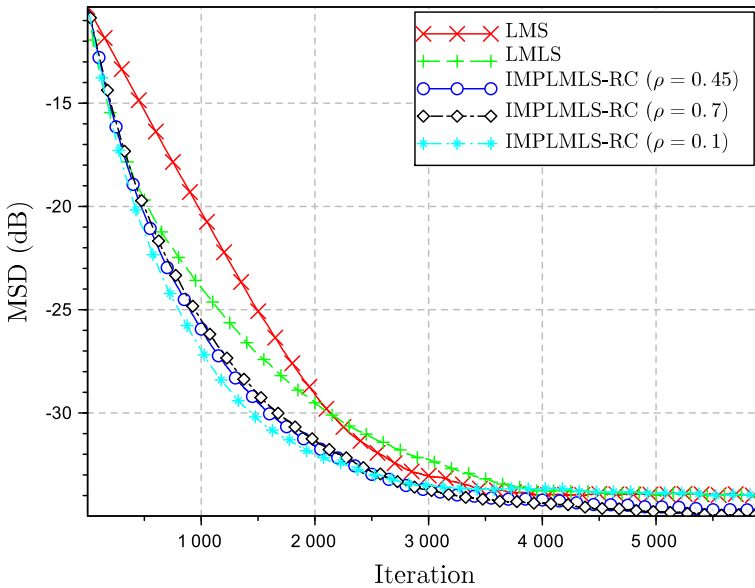


Fig. 4 Comparisons among the LMS, LMLS and IMPLMLS-RC algorithms for $L = 2$, $\rho = 0.1$, $\rho = 0.45$ and $\rho = 0.7$

Table 1 Parameters used in the simulations of Fig. 3

Algorithm	β	α	ρ	L
LMS	1.2×10^{-3}	–	–	–
LMLS	2.5×10^{-2}	1	–	–
IMPLMLS-RC	0.45	4.5	0.45	2; 5; 10

Table 2 Parameters used in the simulations of Fig. 4

Algorithm	β	α	ρ	L
LMS	1.2×10^{-3}	–	–	–
LMLS	2.5×10^{-2}	1	–	–
IMPLMLS-RC	0.45	4.5	0.1; 0.45; 0.7	2

Table 3 Convergence iteration numbers for the simulations shown in Figs. 3 and 4

Algorithm	Iteration
LMS	4263
LMLS	4347
IMPLMLS-RC ($L = 2; \rho = 0.45$)	4812
IMPLMLS-RC ($L = 5; \rho = .45$)	5647
IMPLMLS-RC ($L = 10; \rho = 0.45$)	5936
IMPLMLS-RC ($L = 2; \rho = 0.1$)	3683
IMPLMLS-RC ($L = 2; \rho = 0.7$)	5550

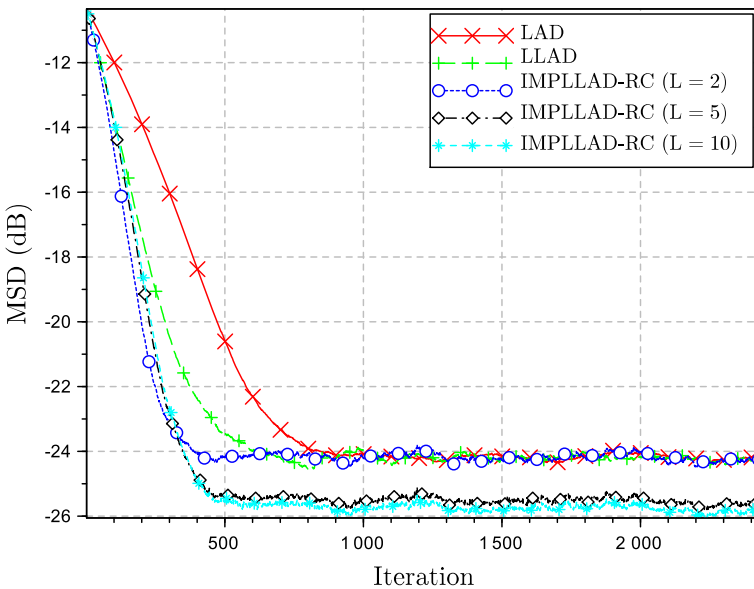


Fig. 5 Comparisons among the LAD, LLAD and IMPLLAD-RC algorithms for $\rho = 0.45$, $L = 2$, $L = 5$ and $L = 10$

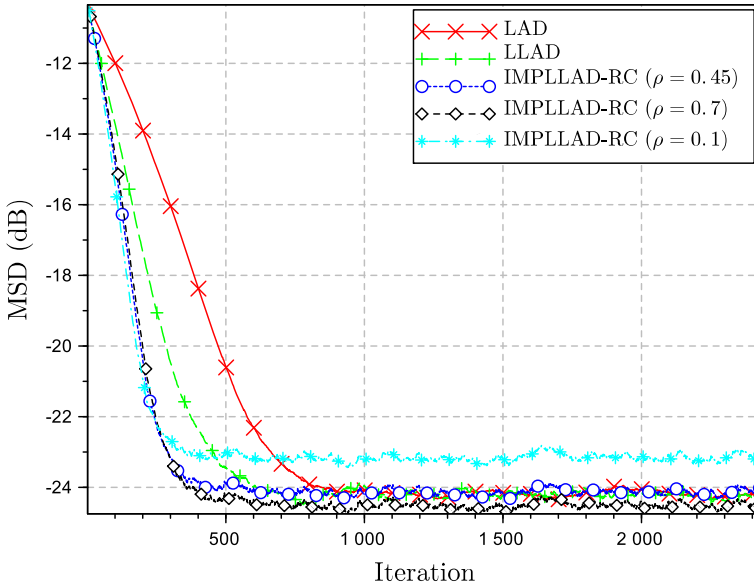


Fig. 6 Comparisons among the LAD, LLAD and IMPLLAD-RC algorithms for $L = 2$, $\rho = 0.1$, $\rho = 0.45$ and $\rho = 0.7$

Table 4 Parameters used in the simulations of Fig. 5

Algorithm	β	α	ρ	L
LAD	8×10^{-4}	–	–	–
LLAD	5×10^{-3}	2	–	–
IMPLLAD-RC	0.32	3	0.45	2; 5; 10

Table 5 Parameters used in the simulations of Fig. 6

Algorithm	β	α	ρ	L
LAD	8×10^{-4}	–	–	–
LLAD	5×10^{-3}	2	–	–
IMPLLAD-RC	0.32	3	0.1; 0.45; 0.7	2

steady-state performance for all algorithms. Simulation results with $L = 5$ and $L = 10$ are presented in Fig. 5. It can be seen that larger values of L improve the steady-state MSD without significantly affecting the convergence rate. Results for $\rho = 0.1$ and $\rho = 0.7$ are shown in Fig. 6. It can be noted that as ρ increases, a slight improvement on steady-state MSD occurs, while for smaller values of ρ there is a negligible gain in convergence speed and poor steady-state performance. The iteration number for which the MSE of each algorithm of Figs. 5 and 6 has converged is shown in Table 6.

Table 6 Convergence iteration numbers for the simulations shown in Figs. 5 and 6

Algorithm	Iteration
LAD	973
LLAD	696
IMPLLAD-RC ($L = 2; \rho = 0.45$)	593
IMPLLAD-RC ($L = 5; \rho = 0.45$)	681
IMPLLAD-RC ($L = 10; \rho = 0.45$)	714
IMPLLAD-RC ($L = 2; \rho = 0.1$)	500
IMPLLAD-RC ($L = 2; \rho = 0.7$)	561

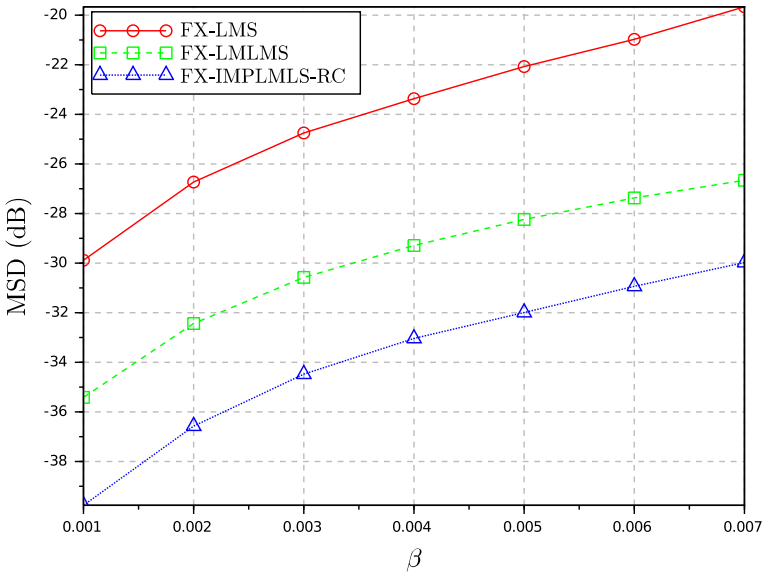


Fig. 7 Steady-state MSD (in dB) for the ANC experiment

5.2 Active Noise Control

Since the advanced algorithm can also be used in ANC applications, some results in this context are presented in this section. The simulated ANC scenario (see Fig. 2) employs the following ideal transfer function:

$$w_n^* = \begin{cases} 1, & \text{for } n = 0 \\ 0, & \text{otherwise} \end{cases}$$

and $N = 20$. The secondary transfer function is given by

$$B(z) = 1 - 0.8z^{-1} + 0.6z^{-2} - 0.4z^{-3} + 0.2z^{-4},$$

and the variance of the white Gaussian additive noise is $\sigma_v^2 = 0.1$.

Table 7 Parameters used in the simulations of Figs. 7 and 8

Algorithm	α	ρ	L
FX-LMS	–	–	–
FX-LMLS	1	–	–
FX-IMPLMLS-RC	1	0.9	5

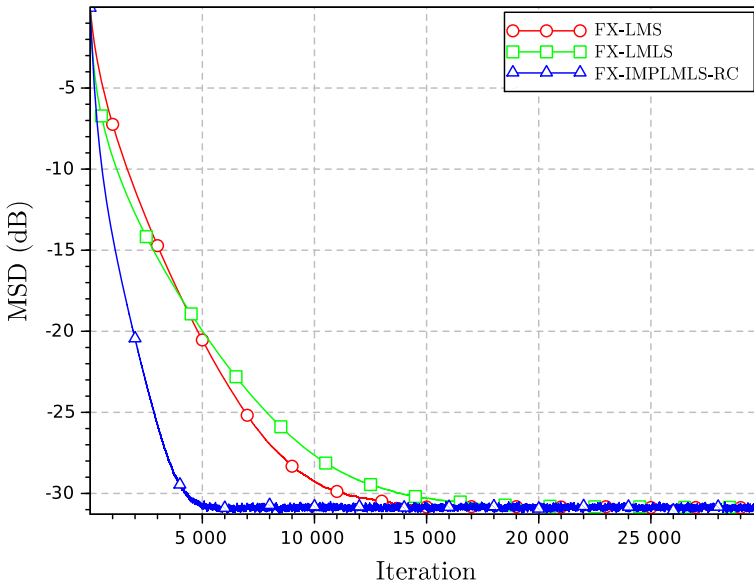
**Fig. 8** MSD (in dB) evolution for the ANC experiment for the FX-LMS (with $\beta = 0.000798$), FX-LMLS (with $\beta = 0.0028$) and FX-IMPLMLS-RC (with $\beta = 0.006$)

Figure 7 presents the steady-state MSD for different β values and other parameters listed in Table 7. This figure shows a clear advantage of the proposed algorithm in the steady-state regime, mainly due to the coefficient reuse strategy.

Figure 8 shows the MSD evolutions of the algorithms when the adaptation step sizes are adjusted to obtain similar steady-state MSD values. The other parameters used in this experiment are displayed in Table 7. This figure allows us to conclude that the proposed FX-IMPLMLS-RC algorithm has the fastest convergence rate, since it employs the proportionate adaptation principle.

6 Conclusions

In this work, novel algorithms were derived with the purpose of improving the performance of the original LMLS and LLAD approaches, in both system identification and ANC tasks. The stochastic gradient problem was transformed in a constrained optimization, thereby allowing the introduction of new techniques to the original algorithms. Simulation results show that the proposed algorithms can overcome the

traditional ones with respect to both steady-state performance and robustness against impulsive noise. It was observed that IMPLLAD-RC is capable of producing a convergence rate as good as that of the LAD algorithm, with a lower MSD at steady state. In a future work, we intend to derive a steady-state analysis of the advanced algorithms in both system identification and ANC setups.

Acknowledgements This study was financed in part by the Coordenação de Aperfeiçoamento de Pessoal de Nível Superior—Brasil (CAPES) Finance Code 001 and CNPq—Brazil, Grants 431215/2016-2 and 309861/2017-9.





References

1. T.Y. Al-Naffouri, A.H. Sayed, Transient analysis of data—normalized adaptive filters. *IEEE Trans. Signal Process.* **51**(3), 639–652 (2003)
2. J. Benesty, S. Gay, An improved PNLMS algorithm. in *Proceedings of the IEEE International Conference on Acoustics, Speech and Signal Processing*, (Orlando, 2002), pp. 1881–1884
3. M. Bouchard, Yu. Feng, Inverse structure for active noise control and combined active noise control/sound reproduction systems. *IEEE Trans. Speech Audio Process.* **9**(2), 141–151 (2001)
4. S. Chan, Y. Chu, Performance analysis and design of fxlms algorithm in broadband anc system with online secondary—path modeling. *IEEE Trans. Audio Speech Language Process.* **20**(3), 982–993 (2012)
5. H. Cho, C.W. Lee, S.W. Kim, Derivation of a new normalized least mean squares algorithm with modified minimization criterion. *Signal Process.* **89**(4), 692–695 (2009)
6. S. Elliott, I. Stothers, P. Nelson, A multiple error LMS algorithm and its application to the active control of sound and vibration. *IEEE Trans. Acoust. Speech Signal Process.* **35**(10), 1423–1434 (1987)
7. D.B. Haddad, M.R. Petraglia, Transient and steady-state MSE analysis of the IMPNLMS algorithm. *Digit. Signal Process.* **33**, 50–59 (2014)
8. S.O. Haykin, *Adaptive Filter Theory* (Prentice Hall, New York, 2001)
9. TSG, I.: 15, *Digital network echo cancellers (recommendation)*. Tech. Rep. G. 168, ITU-T (2004)
10. A. Kar, T. Padhi, B. Majhi, M. Swamy, Analysing the impact of system dimension on the performance of a variable-tap—length adaptive algorithm. *Appl. Acoust.* **150**, 207–215 (2019)
11. S.E. Kim, J.W. Lee, W.J. Song, Steady-state analysis of the NLMS algorithm with reusing coefficient vector and a method for improving its performance. in *Proceedings of the IEEE International Conference on Acoustics, Speech and Signal Processing* (Prague, 2011), pp. 4120–4123
12. L. Liu, M. Fukumoto, S. Saiki, An improved Mu-law proportionate NLMS algorithm, in *Proceedings of the IEEE International Conference on Acoustics, Speech and Signal Processing* (Las Vegas, 2008), pp. 3797–3800
13. T. Padhi, M. Chandra, Cascading time-frequency domain filtered-x LMS algorithm for active control of uncorrelated disturbances. *Appl. Acoust.* **149**, 192–197 (2019)
14. T. Padhi, M. Chandra, A. Kar, Performance evaluation of hybrid active noise control system with online secondary path modeling. *Appl. Acoust.* **133**, 215–226 (2018)
15. T. Padhi, M. Chandra, A. Kar, M. Swamy, Design and analysis of an improved hybrid active noise control system. *Appl. Acoust.* **127**, 260–269 (2017)
16. T. Padhi, M. Chandra, A. Kar, M. Swamy, A new hybrid active noise control system with convex combination of time and frequency domain filtered-x LMS algorithms. *Circuits Syst. Signal Process.* **37**(8), 3275–3294 (2018)
17. M.R. Petraglia, D.B. Haddad, New adaptive algorithms for identification of sparse impulse responses—analysis and comparisons, in *2010 7th International Symposium on Wireless Communication Systems (ISWCS)*, (New York, 2010), pp. 384–388
18. R.M.S. Pimenta, L.C. Resende, D.B. Haddad, M.R. Petraglia, N.N. Siqueira, Novo algoritmo proporcional com reúso de coeficientes e seleção de dados. in *Simpósio Brasileiro de Telecomunicações*, (2017), pp. 1–5

19. R.M.S. Pimenta, L.C. Resende, N.N. Siqueira, D.B. Haddad, M.R. Petraglia, Algoritmo NLMS com reúso de coeficientes e compensação de vies para entradas ruidosas. in *XXXVI Simpósio Brasileiro de Telecomunicações e Processamento de Sinais*, (2018), pp. 1–5
20. R.M.S. Pimenta, L.C. Resende, N.N. Siqueira, I.B. Haddad, M.R. Petraglia, A new proportionate adaptive filtering algorithm with coefficient reuse and robustness against impulsive noise. in *2018 26th European Signal Processing Conference (EUSIPCO)*, (2018), pp. 465–469
21. L.C. Resende, D.B. Haddad, M.R. Petraglia, A variable step-size NLMS algorithm with adaptive coefficient vector reusing. in *2018 IEEE International Conference on Electro/Information Technology (EIT)*, (2018), pp. 0181–0186
22. L.C. Resende, D.B. Haddad, G. d. R. Ferreira, P.H. Campelo, M.R. Petraglia, Sparsity-aware reuse of coefficients normalised least mean squares. *Electron. Lett.* **55**(9), 561–563 (2019)
23. L.C. Resende, N.N. Siqueira, R.M.S. Pimenta, D.B. Haddad, M.R. Petraglia, LMS algorithm with reuse of coefficients and robustness against impulsive noise. in *XXII Congresso Brasileiro de Automática*, (2018), pp. 1–5
24. A.H. Sayed, *Adaptive Filters*, 1st edn. (Wiley, New Jersey, 2011)
25. M.O. Sayin, N.D. Vanli, S.S. Kozat, A novel family of adaptive filtering algorithms based on the logarithmic cost. *IEEE Trans. Signal Process.* **62**(17), 4411–4424 (2014)
26. M.O. Sayin, N.D. Vanli, S.S. Kozat, Improved convergence performance of adaptive algorithms through logarithmic cost. *2014 IEEE International Conference on Acoustics, Speech and Signal Processing (ICASSP)*, (IEEE, Florence, Italy, 2014), pp. 4513–4517
27. H.C. Shin, A.H. Sayed, Mean-square performance of a family of affine projection algorithms. *IEEE Trans. Signal Process.* **52**(1), 90–102 (2004)
28. E. Walach, B. Widrow, The least mean fourth (LMF) adaptive algorithm and its family. *IEEE Trans. Inf. Theory* **30**(2), 275–283 (1984)
29. Y. Xiao, J. Wang, A new feedforward hybrid active noise control system. *IEEE Signal Process. Lett.* **18**(10), 591–594 (2011)
30. N.R. Yousef, A.H. Sayed, A unified approach to the steady-state and tracking analyses of adaptive filters. *IEEE Trans. Signal Process.* **49**(2), 314–324 (2001)

Publisher's Note Springer Nature remains neutral with regard to jurisdictional claims in published maps and institutional affiliations.

Affiliations

José V. G. de Souza¹  · Diego B. Haddad²  · Felipe da R. Henriques²  ·
Mariane R. Petraglia³ 

✉ Mariane R. Petraglia
mariane@pads.ufrj.br

José V. G. de Souza
josevictor.souza@yahoo.com

Diego B. Haddad
diego.haddad@cefet-rj.br

Felipe da R. Henriques
felipe.henriques@cefet-rj.br

¹ Centro Federal de Educação Tecnológica Celso Suckow da Fonseca, Maracanã, RJ, Brazil

² Centro Federal de Educação Tecnológica Celso Suckow da Fonseca, Petrópolis, RJ, Brazil

³ Programa de Engenharia Elétrica, Instituto Alberto Luiz Coimbra de Pós-Graduação e Pesquisa de Engenharia, Universidade Federal do Rio de Janeiro, Rio de Janeiro, RJ 21945-970, Brazil

Reproduced with permission of copyright owner.
Further reproduction prohibited without permission.